Chi Ma,[1] Tuo Ji,[2] Christopher G. Robertson,[3] R. Rajeshbabu,[4] Jiahua Zhu,[2] and Yalin Dong[1,5]

Effect of Filler–Polymer Interface on Elastic Properties of Polymer Nanocomposites: A Molecular Dynamics Study

REFERENCE: Ma, C., Ji, T., Robertson, C. G., Rajeshbabu, R., Zhu, J., and Yalin, D., **"Effect of Filler–Polymer Interface on Elastic Properties of Polymer Nanocomposites: A Molecular Dynamics Study,"** *Tire Science and Technology*, TSTCA, Vol. 45, No. 3, July–September 2017, pp. 227–241.

ABSTRACT: A coarse-grained model has been built to study the effect of the interfacial interaction between spherical filler particles and polymer on the mechanical properties of polymer nanocomposites. The polymer is modeled as bead-spring chains, and nano-fillers grafted with coupling agent are embedded into the polymer matrix. The potential parameters for polymer and filler are optimized to maximally match styrene-butadiene rubber reinforced with silica particles. The results indicated that, to play a noticeable role in mechanical reinforcement, a critical value exists for the grafting density of the filler–polymer coupling agent. After reaching the critical value, the increase of grafting density can substantially enhance mechanical properties. It is also observed that the increase of grafting density does not necessarily increase the amount of independent polymer chains connected to fillers. Instead, a significant amount of increased grafting sites serve to further strengthen already connected polymer and filler, indicating that mechanical reinforcement can occur through the locally strengthened confinement at the filler–polymer interface. These understandings based on microstructure visualization shed light on the development of new filler polymer interfaces with better mechanical properties.

KEY WORDS: molecular dynamics model, filled polymer, filler–polymer coupling agent, mechanical reinforcement

Introduction

Although it has become a routine technique in industry to reinforce rubber's mechanical properties through adding carbon black or silica fillers, the underlying molecular origins for these reinforcements remain unknown or controversial, mainly due to the tremendous difficulties in directly measuring the atomic level events [*1–4*]. The missing knowledge link between molecular structure and macroscopic-level mechanical behaviors hinders rapid and efficient design of new filler–polymer composites. Over the past decades, the industry community heavily relies on experience and trial-and-error methods.

[1] Department of Mechanical Engineering, The University of Akron, Akron, Ohio 44325, USA
[2] Intelligent Composites Laboratory, Department of Chemical and Biomolecular Engineering, The University of Akron, Akron, Ohio 44325, USA
[3] Cooper Tire & Rubber Company, 701 Lima Avenue, Findlay, Ohio 45840, USA
[4] Apollo Tyres Ltd., Oragadam, Sriperumbudur 602105, Tamilnadu, India
[5] Corresponding author. Email:ydong@uakron.edu

There is an urgent need to bridge the knowledge gap through theory and modeling.

Molecular dynamics (MD) simulation, as one kind of molecular model, is the most promising tool to accomplish this goal. MD starts from Newtonian dynamics of each single atom and therefore is able to capture molecular structure and dynamic behavior of a filler–polymer system. In addition, the interatomic interactions are introduced through ready-made empirical potentials so that a considerably large size can be constructed (up to micrometer) and the simulation time can reach up to microsecond. Despite the time and size gaps between current MD simulation and real scenarios, the fundamental features of filler–polymer system can still be captured. It has been widely recognized that the filler–polymer interface plays an important role in mechanical reinforcement. In the tire industry, the filler size is approaching the nanometer scale ($\geq$10 nm [*5*]), a size that can be modeled in an MD simulation. When plastic deformation or other unique properties such as Mullins effect and Payne effect [*6*] occur, chemical or physical bonding ruptures [*7*] at the filler–polymer interface are essential for these irreversible processes. The time scale for bonding rupture and formation is on the order of femtoseconds and can also be appropriately described in an MD simulation. Hence, MD simulation has become a powerful tool to provide atomic insight for filler–polymer micromechanics. For example, to interpret stress softening in Mullin's effect, different micro-level mechanisms have been proposed such as bond rupture [*7*,*8*], molecular slipping [*9*], disentanglement [*10*] of polymer chains, and the double layer model [*11*], which invites further explorations using molecular models. Finite element modeling (FEM) of rubber has been widely used in the tire industry. The formulation of reliable constitutive relations for filler–polymer composites in the context of continuum mechanics is the key for the success of FEM. It was recently revealed the localized strain concentration around nanoparticles can reach to 200% [*12*] under a macro-level strain of 15%, which cannot be properly predicted by conventional FEM. Tang et al. [*13*] has proposed a two-scale constitutive relation to address this issue by arguing that the mechanical response of filler–polymer composites originates from two sources: the filled polymer network and free chains. This new phenomenological constitutive law successfully predicts the over-strain in filled rubber; however, it is in lack of physical evidence for the existence of free chains around fillers [*13*]. Molecular level information is required to provide atomic level validation. With many similar issues remaining unsolved, in conjunction with the rapid development of computational hardware, we have seen continuous efforts to use MD simulation to investigate filler–polymer composites and explain the micromechanics of nanocomposite materials.

A full atomic model [*14*,*15*] has been built to investigate the mechanical properties of filler–polymer composites. Its advantage comes from its full resolution of atomic details so that it can better represent the atomic structure in

polymer chains. However, it suffers from its modeling size: usually, only one filler can be included due to its computational cost. A coarse-grained (CG) model then finds its way into the modeling of the filler–polymer system [*16–18*]. The CG method treats a repeating atom cluster (monomer) as a single bead and neglects atomic features inside the monomer; therefore, it is able to substantially scale up simulation time and model size. Considering the fact that it is the filler–polymer interface that plays the pivotal role in mechanical reinforcement, the sacrifice of atomic features of the monomer chain is reasonable. Fruitful results have been achieved through these two methods. Using a molecular model, it has been demonstrated that the decrease of filler size as well as the increase of interaction between filler and polymer can considerably increase the Young's modulus of filler–polymer composites [*19*,*20*]. Also through a molecular model, the low mobility of polymer around filler was observed during elongation [*21*], and a layer with high chain density near the filler surface was reported [*22*]. Both simulations are consistent with the experimental observation of distinctive mechanical properties in the filler–polymer interfacial region [*23*]. To study the effect of filler dispersion, multi-filler systems were also investigated through the CG method. For example, it was found that the alignment of nano-rods can affect the elastic property of filled polymer [*24*]. Despite these interesting discoveries through an MD simulation, many underlying mechanisms remain unclear due to the complexity of filler–polymer system. For example, in past decades, using silane to functionalize filler to achieve better filler–polymer interactions has won popularity in the tire industry. The use of silane introduces more complexity to the modeling, and the explicit inclusion of silanes in molecular model is rare. We also notice most modeling works in the literature apply tensile deformation by deforming all atoms uniformly. Although the uniform deformation simplifies the calculation, it also imposes unphysical processes into the simulation, considering inhomogeneity is the hallmark of the filler–polymer interface [*24–26*]. In this work, we develop a CG model for a filler–polymer system in which silane molecules are modeled as generic linkers to connect filler and polymer. A more realistic elongation method to generate a stress–strain curve is used in this research so that inhomogeneity at the interface can be well captured. After obtaining a reliable molecular model, the study focuses on the effect of silane, more specifically, the grafting density effect on the elasticity of filled styrene-butadiene rubber (SBR). The microstructure evolution around filler with atomic level information is presented to interpret mechanical reinforcement.

We arrange the paper as follows. We have a detailed introduction about the molecular model, including how to build the filler–polymer system for SBR and how to develop the interatomic potentials. Then, we validate our model by comparing simulation with experiment from the literature. Effects of temperature and cross-link amount on the tensile behavior of unfilled polymer

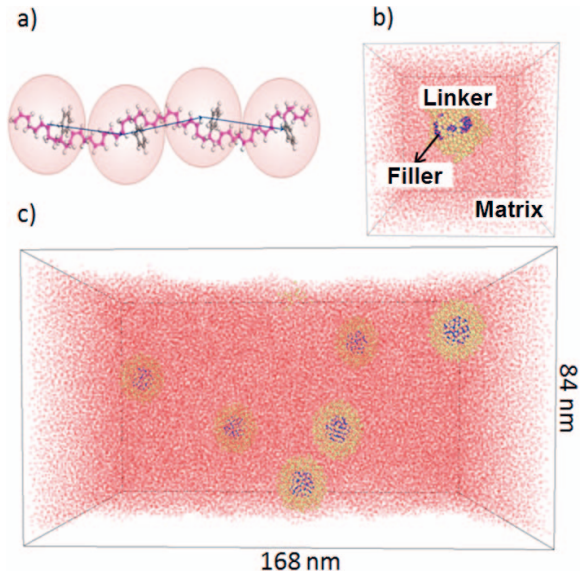

FIG. 1 — *(a) Bead-spring model for SBR polymer. (b) Polymer matrix (red) embedded with single filler (blue) through linkers (yellow). (c) Polymer matrix embedded with multiple fillers, which are used for the mechanical test.*

are investigated first. After validation, we study the elastic reinforcement mechanism of filled SBR rubber in the presence of silane.

Methodology

We use a CG model to simulate the SBR nanocomposite. There are three essential elements: polymer chains, filler, and silane. The bead-spring model is used to mimic the SBR. The basic repeating block, a monomer, consists of two chemical units: styrene (23.5% in mass ratio) and butadiene (76.5%) [*27*]. In the bead-spring model, a spherical bead represents one SBR monomer $C_{21}H_{30}$ that connects to its adjacent beads through covalent bonds (modeled harmonic springs). The bead-spring model of the SBR chain segment is illustrated in Fig. 1a. Silica and carbon black are often used as filler in SBR. The filler takes the regular polygon shape, and its size approaches the nanometer scale (usually $\geq$5 nm). Spherical silica filler with a diameter of 10 nm is then modeled in our simulation. Figure 1b illustrates single silica filler embedded in a polymer matrix. Silane molecules modeled by generic linkers are used to bridge the filler and its surrounding polymer. Generic linkers chemically bond to filler and polymer. The modeled filler (blue), generic linkers (yellow), and polymer (red)

TABLE 1 — *Parameters of L-J potential.*

	Polymer–polymer	Linker–linker	Filler–linker	Linker–polymer	Filler–polymer	Filler–filler
ε	1.0	1.0	0.4	1.0	0.4	0.1
σ	1.0	1.0	1.0	1.0	1.0	0.25
r_c	2.24	2.24	2.24	2.24	2.24	0.56

are shown in Fig. 1b, and the nanocomposite bar used to conduct mechanical measurement is illustrated in Fig. 1c.

There are two categories of interatomic interaction in a filler–polymer system. The adjacent monomers in one polymer chain are connected through a covalent bond. The harmonic potential for the attractive force, in conjunction with Lennard–Jones (LJ) potential mainly for the repulsive force, is used to represent the covalent bond, whose form is expressed as

$$E = K(r - r_0)^2 + 4\varepsilon\left[\left(\frac{\sigma}{r}\right)^{12} - \left(\frac{\sigma}{r}\right)^{6}\right], \tag{1}$$

where the balance distance of harmonic potential $r_0 = 0.98$ and its compliance $K = 420$. σ and ε use the same values as those in L-J potential for polymer–polymer interaction as shown in Table 1. Generic linkers serve as a bridge between the filler and the polymer, and they also connect with the filler and the polymer through a covalent bond whose stiffness is the same as that of the polymer bond. For those without chemical bonding, the long-range van der Waals force dominates the interaction. The L-J potential described below is adopted for the long-range interaction

$$E = 4\varepsilon\left[\left(\frac{\sigma}{r}\right)^{12} - \left(\frac{\sigma}{r}\right)^{6}\right] r < r_c, \tag{2}$$

where r_c denotes cutoff distance and r is the distance between two monomers. σ and ε represent length and energy parameters, respectively. Table 1 exhibits nondimensional parameters of the L-J potential between linkers and linkers, filler and linkers, linkers and polymer, filler and polymer, polymer and polymer, and filler and filler. It is worth mentioning that single filler is treated as a rigid body in the simulation. It is allowed to translate and rotate. However, there is no internal freedom within the filler. Considering the fact that silica and carbon black, typical fillers used in rubber, are much harder than polymer, the rigid assumption is reasonable.

The random walk method is used to generate a polymer matrix. The head monomer of the polymer chain is randomly generated in the simulation box. Starting from the seed monomer, the subsequent monomers are generated following the rule that adjacent monomers have a minimum distance $r_0 = 1\sigma_0$, and there are no overlaps between three sequential monomers. Cross-linkers are

added into polymer in such way that each cross-linker connects two different polymer chains. To embed fillers into the system, we first randomly select initial points and expel a spherical space larger than the filler size by using a virtual atom. We then insert the fillers grafted with linkers into the system and run the system to reach equilibrium. After that, we find the nearest monomer for each linker and connect them. With another equilibrium, the nanocomposite system is ready for a mechanical test.

We use a large-scale atomic/molecular massively parallel simulator code [*28*] to implement the CG model. A dimensionless unit is adopted. To correlate the CG model with an actual material, three basic units should be specified. To model SBR, the mass unit m_0, energy unit ε_0, and length unit σ_0 are set as 282 g/mol, 3 kJ/mol, and 2 nm separately. The energy unit is obtained from the activation energy of two nonbonded SBR monomers that are described in detail in the following section. For the system we are using, there are 400 beads on each chain and 300 polymer chains in total. The system goes through an isothermal-isobaric (NPT) process with $P^* = 0$ and $T^* = 1$ until there is no noticeable dimension variation. After equilibrium, the dimension of the filler–polymer model is 168 nm $\times$ 84 nm $\times$ 84 nm. To conduct the tensile test, we fix one end of the polymer bar and stretch the other end. During elongation, free boundary conditions are applied on all surfaces.

Results and Discussion

Interatomic Potentials

To get potential parameters for the CG model, we run a full atomic model using consistent valence force field (CVFF) [*29*] as the reference. CVFF is an empirical potential for protein and organic molecules whose parameters are derived from the first principles calculation. To characterize the energy parameters in the L-J potential between polymer monomers, we construct two SBR monomers and measure the potential energy as a function of the separating distance by using the CVFF potential. To make our measurement statistically sound, we also rotate one monomer with angles of 90 and 180°, respectively. The average activation energy based on different configurations is used to characterize the long-range van der Waals force, and the energy parameter of polymer–polymer L-J potential is obtained as $\varepsilon_{pp} \approx 3$ kJ/mol. We also characterize the bonding energy between two adjacent monomers in the same chain. A carbon–carbon double bond (sp2) is constructed using CVFF, and the potential energy is mapped out as shown in Fig. 2. The harmonic potential is then fitted to it by adjusting the stiffness parameter K. We notice that it is impossible to have a perfect fitting over the whole distance range through a harmonic potential. Thus, we only focus on the equilibrium regime, the potential well. It is reasonable because molecules tend to reside and vibrate in equilibrium states, and mechanical stimulation only causes small perturbation

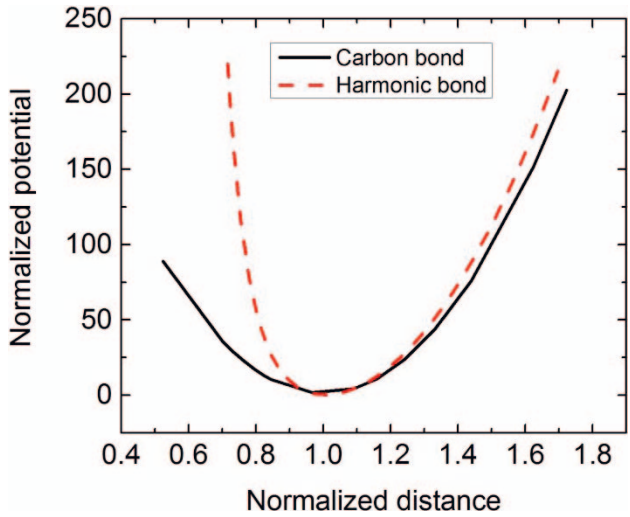

FIG. 2 — *Normalized carbon bond and harmonic bond.*

around the potential well most of the time. The fitted harmonic potential curve is plotted in Fig. 2 (red dashed line) with $K = 420$ (0.523 N/m), meaning the strength of the harmonic bond is approximately 110 times of that of the L-J potential. It is worth pointing out that we deliberately avoid using the real carbon–carbon bonding distance in the harmonic because each bead in our model represents a cluster of atoms. Considering that we are modeling an equivalent bonding, the equilibrium bond length is set as $r_0 = \sigma_0(2\text{ nm})$.

Effect of Cross-Link Density

After obtaining potential parameters for our system, we then examine the effect of cross-link density on stress–strain behavior. In the tire industry, vulcanization is a necessary chemical process by adding sulfur molecules to cross-link polymer chains, thereby giving rise to a more durable network. One direct outcome of vulcanization is the increase of Young's modulus. We use this well-known fact to validate our model. After vulcanization, the cross-linked polymer matrix without filler is stretched up to 300% strain, and the snapshots at different strains can be seen in Fig. 3c. Because we are using free boundary conditions on all directions, we can see the formation of necking, which matches the experimental observation. We also plot the engineering stress–strain curve in Fig. 3a and compare it with the curve from the experiment, as shown Fig. 3b. In the experiment [*30*], the unfilled SBR polymer (20 mm $\times$ 4 mm $\times$ 2 mm) bar containing 1.2 parts per hundred of sulfur was stretched. The tensile behavior of the CG model matches qualitatively well with the

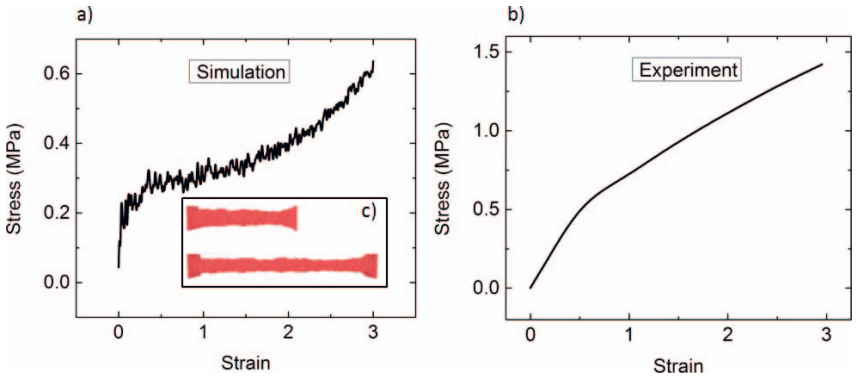

FIG. 3 — *(a) Simulation result of cross-linked polymer where sulfur weight fraction is 0.9%. (b) Experimental result from literature (unfilled SBR) [30]. (c) Snapshot of stretched cross-linked polymer at strain 150% (top bar) and strain 300% (bottom bar).*

experiment (Fig. 3). Note that we do not aim at achieving quantitative-level accuracy considering the simplification of our model. The match in trend between simulation and experiment meets the requirement.

The amount of cross-links significantly affects the tensile behavior of polymer materials. Increasing the amount of cross-links enhances the tensile strength. It reduces the flexibility of polymer chains, and then it requires larger force to stretch the system [*31*]. We conduct tensile tests with different amounts of cross-links in our model. As shown in Fig. 4, the tensile strength is enhanced with the increase of cross-link density. We also compare the simulation results with the experiment from Berriot et al. [*31*]. In the experimental work, the tensile tests were conducted on SBR specimens containing different weight

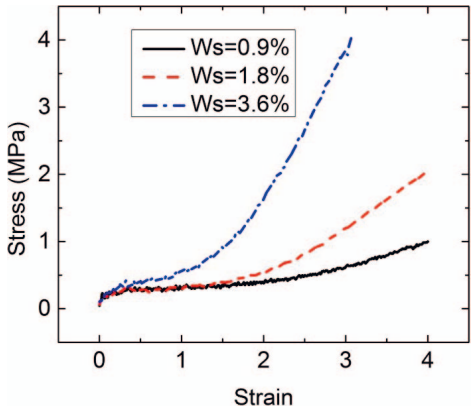

FIG. 4 — *Tensile behavior of polymer model with different cross-link densities.*

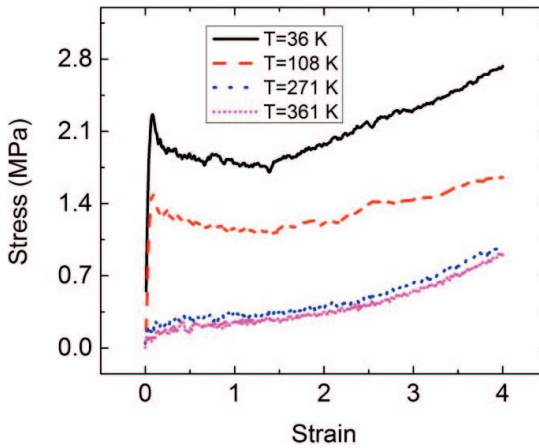

FIG. 5 — *Effect of temperature on stress–strain behavior.*

fractions of sulfur. A similar trend is observed; that is, increasing the sulfur fraction increases the cross-link density, leading to stress enhancement.

Effect of Temperature on Tensile Behavior of Cross-Linked Polymer

Polymer materials exhibit distinctive behaviors under different temperatures. Below the glass-transition temperature (T_g), it is in a glassy state, whereas above the T_g, the polymer is in a rubber state. When used in a tire, SBR is in the rubber state. We need to characterize the state of the filler–polymer system used in the model before running meaningful tests.

Figure 5 shows the tensile test results of the cross-linked polymer matrix at different temperatures. Two distinctive trends can be observed, indicating there is a transition from a glassy to a rubber state. At low temperature (glassy state), the increasing rate of stress is much higher at the initial stage, and there exists a yield point that is a typical phenomenon for plastic polymer [*32*]. At high temperature (rubber state), it becomes easier to stretch the SBR bar, and there is no yield point. The difference originates from the chain entanglements. We know that the microscopic reflection of temperature is the thermodynamic motion of molecules. When in glassy state (low temperature), monomers tend to reside locally so that they cannot overcome the local chain entanglement through thermal motion themselves. Consequently, it requires a larger external force to disentangle the polymer chains. The rubber state, in contrast, is characterized by chain segment motion; thus, it can easily break the chain entanglement through thermal energy. Regardless of the state, when deformation is large enough, rubber experiences a hardening process, indicated by a dramatic increase of stress (Fig. 5). This regime comes from the stretching of the network formed by cross-links.

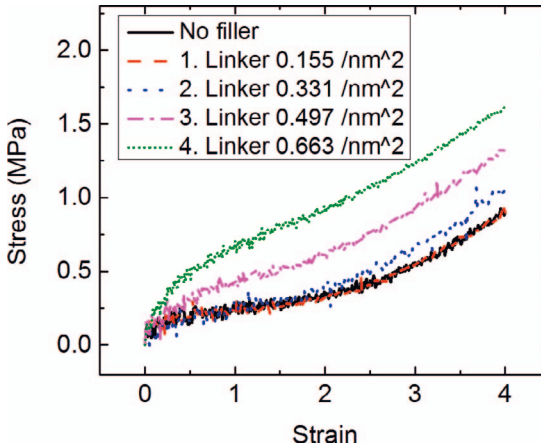

FIG. 6 — *Stress–strain curves of filled polymer and unfilled polymer.*

Effect of Grafting Density

After having a reliable molecular model, we investigate of the effect of the grafting density of silane on the mechanical properties. In industry, to achieve better interaction between filler and polymer, silane coupling agents are routinely used to functionalize the surface of inorganic fillers. Silanes used in tire rubber are bifunctional organic silicon compounds with reactive groups on both ends to form chemical bonds with filler and polymer at the same time. Tetrasulfide, forming two filler–polymer connections in tire compound, is modeled as a generic linker in our simulation. The molecular formula of tetrasulfide is $C_{18}H_{42}O_6Si_2S_4$, with a relative molecular weight of 538 g/mol. Hence, in our model, the molecular weight of one linker is 269 g/mol. The final filler–polymer configuration can be found in Fig. 1c. In the literature, we can see some modeling work focuses on the effect of the interaction strength between filler and polymer [*24*]. However, there is little published work on the grafting density effect of silane. We look at it from a molecular point view. To isolate the grafting density effect from other parameters such as filler interaction and dispersion, we deliberately use a very small amount fraction of filler, six fillers in total, corresponding to a 0.27% volume fraction. In such a case, there is no noticeable interaction between fillers.

Fig. 6 exhibits the stress–strain behavior of the filled polymer at different linker concentrations similar to the chemical bonds between the polymer and silica surface in a real silica-reinforced SBR system. It is found that when the grafting density is low, at 0.155/nm^2 corresponding to 96 linkers, the stress reinforcement is negligible compared to the unfilled polymer case. When the grafting density reaches 0.331/nm^2, corresponding to 205 linkers, the stress reinforcement becomes significant. There is a critical value for the grafting

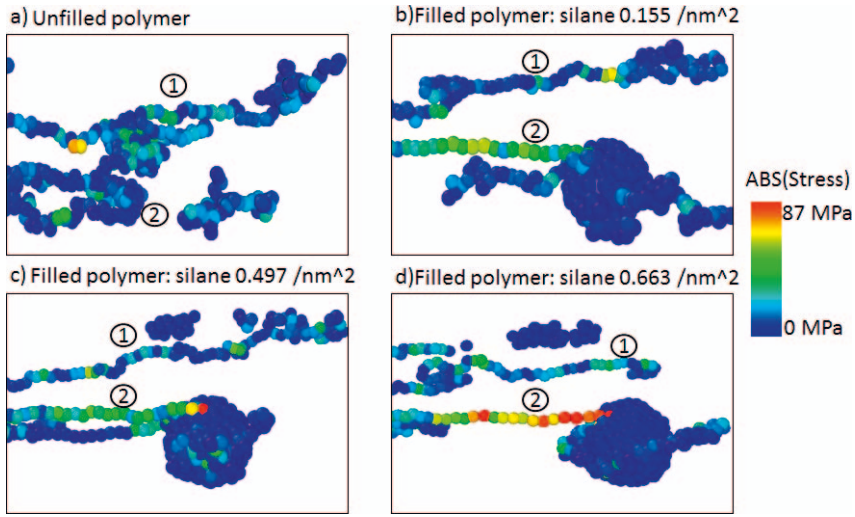

FIG. 7 — *Stress distribution of polymer chains in unfilled polymer and filled polymer at the same 400% strain.*

density of filler–polymer covalent bonds to have an effect on the mechanical reinforcement. In silica-filled SBR tire tread compounds, a typical loading of bis[3-(triethoxysilyl)propyl]tetrasulfide (silane) is 8 wt% relative to the amount of silica. Considering each silane molecule provides two possible filler–polymer connections as mentioned above, this silane concentration translates to 0.312/ nm^2 or 196 potential filler–polymer connections to the spherical silica particle (diameter = 10 nm used in simulation). This value is comparable to the critical linker grafting density determined from the modeling.

We then want to understand the microstructural origin for the mechanical reinforcement. We notice that although for the four cases the numbers of linkers on one filler are increasing, many of them are attached to the same polymer chain but at different grafting sites. As shown in Fig. 7, chain II is bonded to the filler at different sites. By calculation, we find that the averaged amounts of independent polymer chains bonded to one filler are 17, 18, 19, and 19 for the four cases separately, indicating that there is a saturating amount of polymer chains able to grafted to one filler. Therefore, the amount of independent polymer chains bonded to filler is not the reason for the mechanical reinforcement.

To further explore its molecular origin for the reinforcement, we visualize two representative chains in polymer matrix at 400% strain for four cases [one unfilled and three filled cases (0.155, 0.497, and 0.663/nm^2)] as shown in Fig. 7. Chain I is not bonded to any filler, whereas chain II is connected to the filler through linkers. We then calculate the per-atom stress of each monomer as

indicated by its color. It can be seen that there is stress concentration around the filler especially at the bonding site, and the degree of concentration increases with the increase of grafting density. As shown in Fig. 7d, the maximal stress reaches 80 M, whereas the maximal stress in Fig. 7b is around 30 M. As we have calculated, the numbers of grafted independent polymer chains on the filler are similar. Thus, the increased grafting sites are on the same polymer chain, leading to two consequences: (1). it strengthens the interaction between the polymer chain and the filler, leading to a local reinforcement at these particular sites; and (2) when more sites of one polymer chain are attached to the filler, it reduces the mobility of both the polymer chain itself and all monomers in the vicinity of the filler. Due to the formation of the network characterized by one large-size, low-mobility filler and its branches formed through filler–polymer linkers and sulfur cross-linkers, adding more bonding sites strengthens the network and thus reduces the mobility of the whole interfacial region. Any tendency to stretch the polymer chain in this region requires larger stress. This stress can propagate through the polymer chain into the polymer matrix. It then affects an area much larger than the filler itself and explains the existence of the interfacial region often observed in experiments [*25*]. The model results also confirm the experimental observation that immobilized polymer tends to arise around filler [*33*,*34*] due to filler–polymer attachments. It is also worth mentioning that the volume fraction of filler is unrealistically low, mainly to isolate other parameters. When the volume fraction of filler reaches to the industrial level (10–25%), a filler network connected through grafted polymer chains is formed that further augments the reinforcement.

Conclusions

A CG bead-spring model has been built to investigate the molecular origins for the mechanical reinforcement of SBR. We first calculate the potential energy through a full atomic potential and then use these energy values to characterize the interatomic potential for the CG model. To validate our model, the effects of cross-link density and temperature are studied, and the results are compared to published experimental data. Cross-linking (vulcanization) is a very mature technique in experiment to improve the durability of polymer, and the model can well capture the mechanical enhancement due to cross-linking. Filled polymer is very sensitive to temperature, leading to a phase transition from a glassy to a rubbery state. The model is able to recognize the transition and regenerate the distinction in their stress–strain behaviors. We also study the effects of the linker grafting density on the stress–strain behavior of filled SBR. The increase of grafting density can significantly enhance mechanical behavior. It is revealed that the increased graft density does not increase the number of grafted polymer chains. In fact, there is saturating amount of independent

grafted polymer chains on one filler. The increase of linkers only gives rise to more grafting sites for the same polymer chain. Adding more grafting sites for the same polymer chain increases the interacting strength on these specific sites (a local effect), and more importantly, reduces the mobility of the interfacial region through the network centered at the filler and branched by filler–polymer linkers and cross-linkers (an augment effect). These two effects synergistically account for the mechanical reinforcement in filled polymer. Our findings provide molecular evidence for the effects of the filler–polymer interface on the mechanical reinforcement of polymer nanocomposites.

Acknowledgments

The authors are grateful to NSF Center for Tire Research (CenTiRe) for its support. The views presented are those of the collaborative CenTiRe-funded project and not those of any one individual.

References

[*1*] J. Liu, Gao, Y., Cao, D., Zhang, L., and Guo, Z., "Nanoparticle Dispersion and Aggregation in Polymer Nanocomposites: Insights from Molecular Dynamics Simulation," *Langmuir*, Vol. 27, 2011, pp. 7926–7933.

[*2*] B. Meissner and Matějka, L., "Description of the Tensile Stress–Strain Behaviour of Filler-Reinforced Rubber-Like Networks Using a Langevin-Theory-Based Approach. Part II," *Polymer (Guildf)*, Vol. 41, 2000, pp. 7749–7760.

[*3*] J. Diani, Fayolle, B., and Gilormini, P., "A Review on the Mullins Effect," *European Polymer Journal*, Vol. 45, 2009, pp. 601–612.

[*4*] G. M. Odegard, Clancy, T. C., and Gates, T. S., "Modeling of the Mechanical Properties of Nanoparticle/Polymer Composites," *Polymer (Guildf)*, Vol. 46, 2005, pp. 553–562.

[*5*] H. Yagyu and Utsumi, T., "Coarse-Grained Molecular Dynamics Simulation of Nanofilled Crosslinked Rubber," *Computational Materials Science*, Vol. 46, 2009, pp. 286–292.

[*6*] L. Chazeau, Brown, J. D., Yanyo, L. C., and Sternstein, S. S., "Modulus Recovery Kinetics And Other Insights into the Payne Effect for Filled Elastomers," *Polymer Composites*, Vol. 21, 2000, pp. 202–222.

[*7*] A. F. Blanchard and Parkinson, D., "Breakage of Carbon-Rubber," *Industrial and Engineering Chemistry*, Vol. 44, 1952, pp. 799–812.

[*8*] F. Bueche, "Molecular Basis for the Mullins Effect," *Rubber Chemistry and Technology*, Vol. 34, 1961, pp. 493–505.

[*9*] R. Houwink, "Slipping of Molecules during the Deformation of Reinforced Rubber," *Rubber Chemistry and. Technology*, Vol. 29, 1956, pp. 888–893.

[*10*] D. E. Hanson, Hawley, M., Houlton, R., Chitanvis, K., Rae, P., Orler, E. B., and Wrobleski, D. A., "Stress Softening Experiments in Silica-Filled Polydimethylsiloxane Provide Insight into a Mechanism for the Mullins Effect," *Polymer (Guildf)*, Vol. 46, 2005, pp. 10989–10995.

[*11*] Y. Fukahori, "New Progress in the Theory and Model of Carbon Black Reinforcement of Elastomers," *Journal of Applied Polymer Science*, Vol. 95, 2005, pp. 60–67.

[*12*] K. Akutagawa, Yamaguchi, K., Yamamoto, A., Heguri, H., Jinnai, H., and Shinbori, Y., "Mesoscopic Mechanical Analysis of Filled Elastomer with 3D-Finite Element Analysis and Transmission Electron Microtomography," *Rubber Chemistry and. Technology*, Vol. 81, 2008, pp. 182–189.

[*13*] S. Tang, Steven Greene, M., and Liu, W. K., "Two-Scale Mechanism-Based Theory of Nonlinear Viscoelasticity," *Journal of the Mechanics and Physics of Solids*, Vol. 60, 2012, pp. 199–226.

[*14*] Y. Han and Elliott, J., "Molecular Dynamics Simulations of the Elastic Properties of Polymer/Carbon Nanotube Composites," *Computational Materials Science*, Vol. 39, 2007, pp. 315–323.

[*15*] R. Zhu, Pan, E., and Roy, A. K., "Molecular Dynamics Study of the Stress-Strain Behavior of Carbon-Nanotube Reinforced Epon 862 Composites," *Materials Science and Engineering: A*, Vol. 447, 2007, pp. 51–57.

[*16*] F. Müller-Plathe, "Coarse-Graining in Polymer Simulation: From the Atomistic to the Mesoscopic Scale and Back," *ChemPhysChem*, Vol. 3, 2002, pp. 754–769.

[*17*] G. D. Smith, Bedrov, D., Li, L., and Byutner, O., "A Molecular Dynamics Simulation Study of the Viscoelastic Properties of Polymer Nanocomposites," *Journal of Chemical Physics*, Vol. 117, 2002, pp. 9478–9490.

[*18*] R. A. Vaia and Emmanuel, P., "Polymer Nanocomposites: Status and Opportunities," *MRS Bulletin*, Vol. 26, 2001, pp. 394–401.

[*19*] A. Adnan, Sun, C. T., and Mahfuz, H., "A Molecular Dynamics Simulation Study to Investigate the Effect of Filler Size on Elastic Properties of Polymer Nanocomposites," *Composites Science and Technology*, Vol. 67, 2007, pp. 348–356.

[*20*] S. Yu, Yang, S., and Cho, M., "Multi-Scale Modeling of Cross-Linked Epoxy Nanocomposites," *Polymer (Guildf)*, Vol. 50, 2009, pp. 945–952.

[*21*] J. Liu, Wu, S., Zhang, L., Wang, W., and Cao, D., "Molecular Dynamics Simulation for Insight into Microscopic Mechanism of Polymer Reinforcement," *Physical Chemistry Chemical Physics*, Vol. 13, 2011, pp. 518–29.

[*22*] A. Ghanbari, Ndoro, T. V. M., Leroy, F., Rahimi, M., Böhm, M. C., and Müller-Plathe, F., "Interphase Structure in Silica-Polystyrene Nanocomposites: A Coarse-Grained Molecular Dynamics Study," *Macromolecules*, Vol. 45, 2012, pp. 572–584.

[*23*] K. Akutagawa, Yamaguchi, K., Yamamoto, A., and Heguri, H., "Mesoscopic Mechanical Analysis of Filled Elastomer with 3D-Finite Element Anaysis and Transmission Electron Microtomography," *Rubber Chemistry and Technology*, Vol. 81, 2008, p. 182.

[*24*] Y. Gao, Liu, J., Shen, J., Zhang, L., Guo, Z., and Cao, D., "Uniaxial Deformation of Nanorod Filled Polymer Nanocomposites: A Coarse-Grained Molecular Dynamics Simulation," *Physical Chemistry Chemical Physics*, Vol. 16, 2014, pp. 16039–16048.

[*25*] K. Akutagawa and Nishi, T., "The Nanotech Challenge: Creating a Nano-Architecture Design for Tire Materials Development," *Tire Technolology International*, 2013.

[*26*] S. K. Kumar and Krishnamoorti, R., "Nanocomposites: Structure, Phase Behavior, and Properties," *Annual Review of Chemical and Biomolecular Engineering*, Vol. 1, 2010, pp. 37–58.

[*27*] V. Arrighi, McEwen, I. J., Qian, H., and Serrano Prieto, M. B., "The Glass Transition and Interfacial Layer in Styrene-Butadiene Rubber Containing Silica Nanofiller," *Polymer (Guildf)*, Vol. 44, 2003, pp. 6259–6266.

[*28*] S. Plimpton, "Fast Parallel Algorithms for Short-Range Molecular Dynamics," *Journal of Computational Physics*, Vol. 117, 1995, pp. 1–19.

[*29*] P. Hobza, Kabeláč, M., Šponer, J., Mejzlík, P., and Vondrášek, J., "Performance of Empirical Potentials (AMBER, CFF95, CVFF, CHARMM, OPLS, POLTEV), Semiempirical Quantum Chemical Methods (AM1, MNDO/M, PM3), and Ab Initio Hartree-Fock Method for Interaction of DNA Bases: Comparison with Nonempirical beyond Hartree-Fock Results," *Journal of Computational Chemistry*, Vol. 18, 1997, pp. 1136–1150.

[*30*] M. M. Saatchi and Shojaei, A., "Mechanical Performance of Styrene-Butadiene-Rubber Filled with Carbon Nanoparticles Prepared by Mechanical Mixing," *Materials Science and Engineering: A*, Vol. 528, 2011, pp. 7161–7172.

[*31*] A. J. Marzocca and Goyanes, S., "An Analysis of the Influence of the Accelerator/Sulfur Ratio in the Cure Reaction and the Uniaxial Stress–Strain Behavior of SBR," *Journal of Applied Polymer Science*, Vol. 91, 2004, pp. 2601–2609.

[*32*] Y. Li, Yang, T., Yu, T., Zheng, L., and Liao, K., "Synergistic Effect of Hybrid Carbon Nantube–Graphene Oxide as a Nanofiller in Enhancing the Mechanical Properties of PVA Composites," *Journal of Materials Chemistry*, Vol. 21, 2011, p. 10844.

[*33*] J. Berriot, Montes, H., Lequeux, F., Long, D., and Sotta, P., "Evidence for the Shift of the Glass Transition near the Particles in Silica-Filled Elastomers," *Macromolecules*, Vol. 35, 2002, pp. 9756–9762.

[*34*] C. G. Robertson and Rackaitis, M., "Further Consideration of Viscoelastic Two Glass Transition Behavior of Nanoparticle-Filled Polymers," *Macromolecules*, Vol. 44, 2011, pp. 1177–1181.